Int. J. Heat Mass Transfer. Vol. 32, No. 10, pp. 1897–1906, 1989
Printed in Great Britain

0017–9310/89 $3.00 + 0.00

Coupled heat condensation and mass absorption with comparable concentrations of absorbate and absorbent

NEIMA BRAUNER, DAVID MOALEM MARON and HANUCH MEYERSON
Department of Fluid Mechanics and Heat Transfer, Faculty of Engineering, Tel-Aviv University, Ramat Aviv 69978, Israel

(*Received* 21 *October* 1988)

Abstract—Absorption of sparingly soluble gases is conventionally characterized by infinite dilution of absorbate. The present study relates to vapour absorption, where the concentration levels of absorbate and absorbent are comparable (finite dilution of absorbate). Such a process, for instance, is the hygroscopic condensation of cold low pressure vapour on a concentrated hot brine falling film. Isothermal and non-isothermal absorptions are considered. The latter represents coupled heat and mass transfer. It is shown that in the case of finite dilution, the lateral convective term ought to be accounted for. The resulting transfer rates are shown to depend on both the absorbate concentration level and the driving force and are significantly augmented compared to the prediction of Higbie's theory.

1. INTRODUCTION

IN TYPICAL heat transfer condensation the impetus for the process is usually the thermal driving force, requiring the condensing vapour phase to be at a higher thermal level. As such, a degradation of the temperature level in the direction of the vapour condensation is involved.

A different condensation scheme, referred to as hygroscopic condensation, has been recently dealt with in refs. [1, 2], whereby low temperature (low pressure) pure vapour condenses and is absorbed on a relatively hot film of hygroscopic (salt) solution. The condensation occurs due to the reduced vapour pressure of the concentrated salt solution. The driving force for condensation is the difference between the pressure of the vapour phase and the partial pressure of the water component in the brine solution. The condensation, in this case, is governed rather by mass transfer mechanisms with possible opposing thermal forces [3–6].

The interest in condensation of water vapour on concentrated brine stemmed from the search of energy recovery [1, 2, 5, 6]. The (naturally available†) brine, which essentially represents a storage of heat, is used, as a matter of fact, to upgrade low pressure steam. Clearly, the commercial applicability of such a process to energy recovery schemes is highly dependent on the overall transfer rates that can be achieved.

The distinction of hygroscopic condensation compared to vapour condensation on its pure liquid phase or on transferring surfaces is two-fold. The first is the coupling between energy and mass transfer. In utilizing a hygroscopic brine film as the condensing surface, the overall performance is governed by both the thermal resistance and the associated coupled resistance to mass transfer in the brine film, which is continuously diluted by the condensation at the free interface. Inspection of the relevant literature indicates that the focus has been mainly on the problem of liquid phase controlled mass transfer into a liquid film in isothermal conditions. These have been recently reviewed [7–10]. Relatively few studies accounted for the temperature variation. Yih and Seagrave [11] studied the effect of an a priori assumed temperature distribution across a laminar falling film on the physical properties, hence on the absorption process. Nakoryakov and Grigor'eva solved for the temperature profile [12, 13], assuming a uniform velocity across the film. The solutions for the coupled energy and diffusion equations were obtained in the form of eigenfunction series. Analytical solution for the temperature and concentration distribution at the entry region were also presented in ref. [13]. Later on, Grossman [14] improved the above model by eliminating the assumptions of uniform velocity across the film. Grossman and Heath [15] further extended the laminar model to turbulent flow conditions and widely discussed the heat and mass transfer coefficients for various operating conditions.

The second important feature of vapour absorption by concentrated brine is that the concentration levels of the absorbate (usually water) and the solute (salt) are comparable. It is at this point worth noting that most of the previous experimental and theoretical studies have dealt with infinite absorbate dilution, whereby sparingly soluble gases are absorbed into

† Solutions of $CaCl_2$ up to 40–50% by weight are available in the Dead Sea, Israel.

NOMENCLATURE

a_1, a_2	constants in equation (19)
A_1, A_2	integration constants, equation (27)
B_1, B_2	integration constants, equation (28)
c_p	specific heat [kJ kg^{-1} K^{-1}]
C	molar density [mol m^{-3}]
C_A	absorbate concentration [mol m^{-3}]
C_B	absorbent concentration [mol m^{-3}]
D	diffusion coefficient [m^2 s^{-1}]
h	heat transfer coefficient [kJ m^{-2} s^{-1} K^{-1}]
k	thermal conductivity [kJ m^{-1} s^{-1} K^{-1}]
K	mass transfer coefficient [m s^{-1}]
Le	Lewis number, D/α
N	molar flux [mol s^{-1} m^{-2}]
$\mathcal{N}$	non-dimensional molar flux, equation (17)
Nu	Nusselt number, hz/k
P	vapour pressure [N m^{-2}]
Pe	Peclet number, $\frac{3}{8}Re\,Pr$
Pr	Prandtl number, $c_p\mu/k$
Re	film Reynolds number, $4\Gamma/\mu$
Sc	Schmidt number, ν/D
Sh	Sherwood number, Kz/D
T	temperature [K]
u	downstream velocity [m s^{-1}]
U_{max}	interfacial velocity [m s^{-1}]
X_A	molar fraction of absorbate
y	perpendicular direction [m]
Y	non-dimensional perpendicular direction, y/δ
z	downstream direction [m]
Z	non-dimensional direction, $(z/\delta)/Pe$.

Greek symbols

α	thermal diffusivity [m^2 s^{-1}]
β, γ	constants, equation (17)
Γ	liquid flow rate [kg s^{-1} m^{-1}]
δ	film thickness [m]
η	integration variable
θ	non-dimensional temperature, equation (14)
λ^*	molar heat of absorption [kJ kg^{-1} mol^{-1}]
Λ	non-dimensional heat of absorption, equation (18)
μ	viscosity [kg m^{-1} s^{-1}]
ν	kinematic viscosity [m^2 s^{-1}]
ξ	similarity variable, $Y/(4Z)^{1/2}$, equation (22)
ρ	density [kg m^{-3}]
ϕ	non-dimensional absorbate concentration, equation (14)
χ	vapour quality
ψ	function defined in equation (25)
Ω	enhancement factor, equation (49).

Subscripts

A	absorbate
B	non-volatile absorbent
c	condensing vapour
i	at inlet.

Superscripts

*	at equilibrium
–	average
0	infinite dilution.

liquid films, and thus ignore the effect of the absorbate concentration level [7–9]. The others mentioned studies which more specifically dealt with vapour absorption into hygroscopic solutions [10–16], while accounting for the coupling between energy and diffusion, still considered the process as of infinite absorbate dilution.

The present study is essentially aimed at evaluating analytically the effect of the absorbate concentration level in systems of finite absorbate dilution. The study is thus complementary to Brauner and Maron's work on hygroscopic condensation. However, while the previous presentations [1–6] dealt with experimental and general theoretical modelling of the transfer rates, the present study is focused on elucidating the basic mechanisms associated with comparable concentrations of absorbate and absorbent.

2. THE PHYSICAL MODEL AND GOVERNING EQUATIONS

The physical system and coordinates are schematically described in Fig. 1. A concentrated brine of a salt concentration C_{Bi}, water concentration C_{Ai} and temperature T_i, enters the condensation compartment at $z = 0$. It flows down over an inclined surface, in contact with pure stagnant saturated vapour (steam) at constant pressure P_c. The saturation temperature of the condensing vapour $T_c(P_c)$ may be lower than the brine temperature T_i. However, the relatively cold vapour may condense and be absorbed

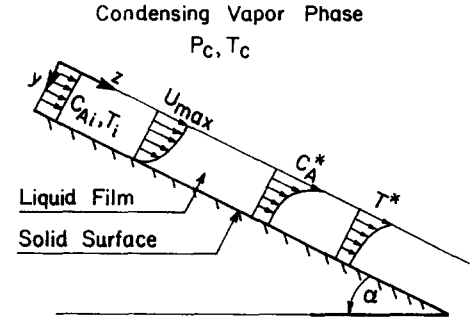

FIG. 1. Schematic description of the physical model and coordinates.

by the brine film, providing the brine vapour pressure $P_A^*(T, C_A)$ is lower than P_c. In the absence of non-condensables, the resistance to absorption in the vapour phase is negligible and a liquid-phase controlled condensation–absorption is considered. Also, heat losses from the liquid phase to the adjacent condensing vapour are ignored. The heat released due to the hygroscopic condensation affects an increase of the brine temperature. Thus coupling between the mass and heat transfer process results.

In formulating the governing equations it is assumed that the vapour absorption rate is small compared to the mass flow rate of the brine film. Therefore, the film thickness, the downstream velocities and the physical properties of the liquid film are considered to be constant. For a fully developed laminar film flow, the well-known Nusselt solution prevails, with the downstream velocity profile $u(y)$ given by

$$u(y) = U_{max}\left[1-\left(\frac{y}{\delta}\right)^2\right] \tag{1}$$

where U_{max} is the interfacial velocity and δ the film thickness.

A differential mass balance on the condensing component reads

$$\frac{\partial N_{Az}}{\partial z} + \frac{\partial N_{Ay}}{\partial y} = 0 \tag{2}$$

where N_{Az}, N_{Ay} denote the molar flux of absorbate A in the z-, y-directions, respectively. Since the axial diffusion contribution to the molar flux is negligible the first component of equation (2) reduces to

$$N_{Az} = -DC\frac{\partial X_A}{\partial z} + X_A(N_{Az}+N_{Bz}) \simeq C_A u(y) \tag{3}$$

where C is the molar density, C_A, X_A the molar concentration and molar fraction of the condensing component and D the diffusion coefficient of the absorbate in the liquid. In the perpendicular direction, y, the molar flux is given by

$$N_{Ay} = -DC\frac{\partial X_A}{\partial y} + X_A(N_{Ay}+N_{By}). \tag{4}$$

The convective term in equation (4) can be omitted for either $X_A \to 0$ or $N_{Ay} = -N_{By}$, neither of which holds in the case of hygroscopic condensation. For instance, the minimum molar fraction of water which corresponds to a saturated salt solution of $MgCl_2$, $CaCl_2$, LiBr, NaOH, is about $X_A \simeq 0.8$. On the other hand, the salt is not transferred, neither through the film free interface, nor through the solid wall, and thus $N_{By} \simeq 0$ may reasonably be assumed. Under these conditions, equation (4) yields

$$N_{Ay} = -\frac{D}{(1-X_A)}\frac{\partial C_A}{\partial y}. \tag{5}$$

For relatively short exposure time (small z) the diffusion boundary layer is limited to the near free interface region and thus, by equation (1), $u(y) \simeq U_{max}$. Substituting equations (3) and (5) into equation (2) yields

$$U_{max}\frac{\partial C_A}{\partial z} = D\frac{\partial}{\partial y}\left[\frac{1}{(1-C_A/C)}\frac{\partial C_A}{\partial y}\right]. \tag{6}$$

In some cases the heat interaction is small and the process may be considered isothermal. Hygroscopic condensation, on the other hand, is characterized by a significantly large heat of absorption. The heat released during the hygroscopic condensation affects an increase in the brine temperature, which influences the equilibrium interfacial concentration at the film free interface and thus a combined heat and mass transfer is to be considered, where the temperature and concentration at the free interface are interrelated through the thermodynamic equilibrium condition.

The energy equation is now simplified under several assumptions, which are reasonably valid for the physical model of Fig. 1. First, viscous dissipation, thermodiffusion effects and the axial heat conduction term are negligible. Also, for a small condensation rate (compared to the average film mass flow rate) the lateral heat convection component is ignored. Moreover, under the condition of short contact time, consistent with equation (6), the energy equation reduces to

$$U_{max}\frac{\partial T}{\partial z} = \alpha\frac{\partial^2 T}{\partial y^2} \tag{7}$$

where α is the solution thermal diffusivity ($\alpha = k/\rho c_p$). The corresponding boundary conditions for equations (6) and (7) are

$$\begin{aligned} &z = 0, \quad C_A = C_{Ai}, \quad T = T_i \\ &y = 0, \quad C_A = C_A^*, \quad T = T^*(P_c, C_A^*) \\ &y \to \infty, \quad C_A = C_{Ai}, \quad T = T_i \end{aligned} \tag{8}$$

where C_A^* is the absorbate interfacial concentration, assuming a vapour pressure equilibrium at the liquid free interface at a temperature level T^* and an external pressure level of the vapour phase, P_c. Note that though C_A^*, T^* are in fact unknown, they are related to each other by both the temperature–concentration–pressure equilibrium

$$P(C_A^*, T^*) = P_c = \text{const.} \tag{9}$$

and the condensation heat flux through the free interface

$$-k\left.\frac{\partial T}{\partial y}\right|_{y=0} = \lambda_c^* N_{Ay}\Big|_{y=0} \tag{10}$$

where $N_{Ay}|_{y=0}$ is the interfacial molar condensation flux as defined by equation (5) and λ_c^* is the molar heat of absorption of the condensing vapour and is a function of the interfacial conditions, C_A^*, T^*. Clearly, equations (9) and (10) represent the coupling between the heat and mass transfer mechanisms.

The non-dimensional presentations of equations (6) and (7) and boundary conditions are

$$\frac{\partial\phi}{\partial Z} = Le\frac{\partial}{\partial Y}\left[\frac{1}{\gamma\phi+\beta}\frac{\partial\phi}{\partial Y}\right] \tag{11}$$

$$\frac{\partial\theta}{\partial Z} = \frac{\partial^2\theta}{\partial Y^2} \tag{12}$$

$$Z=0; \quad \phi=0; \quad \theta=0 \tag{13a}$$

$$Y=0; \quad \phi=\phi^*; \quad \theta=\theta^* \tag{13b}$$

$$Y\to\infty; \quad \phi=0; \quad \theta=0 \tag{13c}$$

where

$$\phi=\frac{C_A-C_{Ai}}{C^*_{Ai}-C_{Ai}}; \quad \theta=\frac{T-T_i}{T_i^*-T_i}; \quad Y=\frac{y}{\delta}; \quad Z=\frac{z}{\delta}\frac{1}{Pe}$$

$$Pe=\frac{3}{8}Re\,Pr; \quad Re=\frac{4\Gamma}{\mu}=\frac{8}{3}\frac{U_{max}\delta}{\nu}; \quad Pr=\nu/\alpha;$$

$$Le=\frac{D}{\alpha}=\frac{Pr}{Sc}; \quad \gamma=(C_{Ai}-C^*_{Ai})/C; \quad \beta=1-C_{Ai}/C. \tag{14}$$

Here, C^*_{Ai} is the equilibrium concentration at the entry temperature, T_i, and vapour pressure, P_c, $C^*_{Ai}=C^*_A(T_i,P_c)$ (and thus represents the interfacial concentration in the case of isothermal absorption). The equilibrium temperature $T_i^*=T^*(C_{Ai},P_c)$ includes the boiling point elevation corresponding to the brine concentration, C_{Ai}, which is in equilibrium with its vapour at pressure, P_c. In fact $T_i^*-T_i$ is a useful measure of the nominal available temperature driving force for the hygroscopic condensation process. Note that, the actual temperature drop T_c-T_i may be negative in the case of hygroscopic condensation, while condensation still takes place.

The dimensionless (unknown) interfacial temperature and concentration, ϕ^* and θ^*, are related to each other by the dimensionless form of equations (9) and (10)

$$P(\phi^*,\theta^*)=\text{const.} \tag{15}$$

$$-\left.\frac{\partial\theta}{\partial Y}\right|_{Y=0}=\Lambda\mathcal{N} \tag{16}$$

where $\mathcal{N}$ is the dimensionless molar flux of condensation at the free interface and Λ the dimensionless heat of condensation–absorption

$$\mathcal{N}=\left.\frac{\delta}{D(C^*_{Ai}-C_{Ai})}N_{Ay}\right|_{y=0}=-\frac{1}{(\gamma\phi^*+\beta)}\left.\frac{\partial\phi}{\partial Y}\right|_{Y=0} \tag{17}$$

$$\Lambda=\frac{Le\,\lambda_c^*(C^*_{Ai}-C_{Ai})}{\rho c_p(T_i^*-T_i)}. \tag{18}$$

In order to proceed with the solution it is necessary to specify an equilibrium relation between temperature composition and vapour pressure (equation (15)). Experimental data, available in the literature for various brines are usually formulated in a linear relation between temperature, composition and the logarithm of the vapour pressure at equilibrium [14]. Thus, under the conditions of constant vapour pressure, P_c, a linear relation specifies

$$C_A^*=a_1T^*+a_2 \tag{19}$$

or, in terms of the dimensionless concentration and temperature defined in equation (14), equation (19) becomes

$$\phi^*+\theta^*=1. \tag{20}$$

The solution also requires data of the latent heat condensation of vapour over the brine interface $\lambda_c^*(C_A^*,T^*)$, which is given by [1, 6]

$$\lambda_c^*=\lambda^*|_{C_A^*,T^*}-c_{pc}(T^*-T_c)-(1-\chi)\lambda \tag{21}$$

where λ^* is the heat of evaporation (or condensation) of a unit mass of pure water from a solution of concentration C_A^* which is in thermodynamic equilibrium with its (superheated) vapour at a temperature T^*. Here, however, the latent heat λ^* is to be first corrected for the sensible heat losses due to condensation of relative cold vapour at temperature $T_c\leqslant T^*$ with a specific heat c_{pc}. The third term of equation (21) represents the latent heat loss due to condensation of vapour of quality, $\chi<1$. For absorption of water vapour the dependence of λ_c^* on C_A^* and T^* is known to be rather weak, and thus the solution is proceeded assuming a constant (specified) λ_c^*.

The partial differential equations, equations (11) and (12), are now reduced to ordinary differential equations by substituting a similarity variable, $\xi=Y/(4Z)^{1/2}$

$$Le\frac{d}{d\xi}\left[\frac{1}{\gamma\phi+\beta}\frac{d\phi}{d\xi}\right]+2\xi\frac{d\phi}{d\xi}=0; \quad \xi=Y/(4Z)^{1/2} \tag{22}$$

$$\frac{d^2\theta}{d\xi^2}+2\xi\frac{d\theta}{d\xi}=0 \tag{23}$$

and the boundary conditions, equations (13), (16), and (20), read

$$\xi\to\infty, \quad \phi=0 \tag{24a}$$

$$\xi\to\infty, \quad \theta=0 \tag{24b}$$

$$\xi=0, \quad \phi^*+\theta^*=1 \tag{24c}$$

$$\xi=0, \quad \frac{d\theta}{d\xi}=\frac{\Lambda}{\gamma\phi+\beta}\frac{d\phi}{d\xi}. \tag{24d}$$

The conditions in equations (24c) and (24d) represent the coupling between the energy and diffusion equations, while the term, $1/(\gamma\phi+\beta)$, in equation (22) evolves due to comparable levels of absorbent and absorbate concentrations.

3. SOLUTION OF THE GOVERNING EQUATIONS

Equations (22) and (23) are now to be solved under the conditions of equations (24). The case of iso-

thermal absorption, where both θ and Λ are identically zero and thus only equation (22) remains, has been recently solved by the authors [18]. The solution proceeds here for the more general case of non-isothermal condensation–absorption as in hygroscopic condensation.

Substituting $\psi = \gamma\phi + \beta$ into equation (22) yields

$$Le\frac{\mathrm{d}}{\mathrm{d}\xi}\left[\frac{\mathrm{d}\ln\psi}{\mathrm{d}\xi}\right] + 2\xi\psi\frac{\mathrm{d}\ln\psi}{\mathrm{d}\xi} = 0; \quad \psi = \gamma\phi + \beta. \tag{25}$$

Equation (25) when multiplied by

$$\exp\left(\int_0^{\xi/\sqrt{(Le)}} 2\xi'\psi(\xi')\,\mathrm{d}\xi'\right)$$

can be easily rearranged into

$$\frac{\mathrm{d}}{\mathrm{d}\xi}\left\{\frac{1}{\psi}\frac{\mathrm{d}\psi}{\mathrm{d}\xi}\exp\left[\int_0^{\xi/\sqrt{(Le)}} 2\xi'\psi(\xi')\,\mathrm{d}\xi'\right]\right\} = 0. \tag{26}$$

Double integration of equation (26) yields

$$\psi(\xi/\sqrt{(Le)}) = \gamma\phi(\xi/\sqrt{(Le)}) + \beta = \exp\left\{A_1\int_0^{\xi/\sqrt{(Le)}} \times\exp\left[-\int_0^{\eta} 2\xi'\psi(\xi')\,\mathrm{d}\xi'\right]\mathrm{d}\eta + A_2\right\}. \tag{27}$$

The solution obtained, as given by equation (27), is a Voltera integral equation. It is well known from functional analysis that this type of equation may be solved by applying an iterative scheme, which turns out to be convergent for any arbitrary initial guess of $\psi(\xi)$ [19]. The unknown constants A_1, A_2 are derived from the boundary conditions in equations (24), which are coupled with the energy equation, equation (23), the solution of which is given by

$$\theta = B_1\,\mathrm{erf}\,(\xi) + B_2. \tag{28}$$

Note that while the temperature solution is obtained in terms of ξ, as in equation (28), the concentration solution is obtained in terms of $\xi/\sqrt{(Le)}$, equation (27). Utilizing the boundary condition of equation (24b) in equation (28), yields

$$B_1 = -B_2. \tag{29}$$

Substituting the ϕ, θ solutions of equations (27) and (28) into equations (24c) and (24d) yields a relationship between A_1 and A_2

$$B_2 + \frac{\exp(A_2) - \beta}{\gamma} = 1 \tag{30}$$

$$B_1 = \frac{\sqrt{\pi}}{2}\frac{\Lambda A_1}{\gamma\sqrt{(Le)}}. \tag{31}$$

Combining equations (29)–(31) and the definitions of β, γ given in equation (14) yields

$$\mathrm{e}^{A_2} = \beta + \gamma + \frac{\sqrt{\pi}}{2}\frac{\Lambda}{\sqrt{(Le)}}A_1 = 1 - \frac{C^*_{Ai}}{C} + \frac{\sqrt{\pi}}{2}\frac{\Lambda}{\sqrt{(Le)}}A_1. \tag{32}$$

Applying boundary conditions (24a) while utilizing equation (32) results in the following relation for A_1:

$$\left(1 - \frac{C^*_{Ai}}{C} + \frac{\sqrt{\pi}}{2}\frac{\Lambda}{\sqrt{(Le)}}A_1\right)\exp \times\left\{A_1\int_0^{\infty}\exp\left[-\int_0^{\eta} 2\xi'\psi(\xi')\,\mathrm{d}\xi'\right]\mathrm{d}\eta\right\} + \left[\frac{C_{Ai}}{C} - 1\right] = 0. \tag{33}$$

Equations (27)–(33) are solved iteratively: starting with a uniform distribution, $\psi(\xi) = 1$, equation (33) is solved for A_1, which in turn is utilized in equations (32) and (27) to obtain a new $\psi(\xi)$ or new $\phi(\xi)$. Equations (28)–(31) then yield the corresponding solutions for $\theta(\xi)$. Less than 10 iterations have been usually found sufficient to yield convergence. Note that the solution is obtained for a given set of C^*_{Ai}/C, C_{Ai}/C and $\Lambda/\sqrt{(Le)}$.

Having established the ϕ, θ solutions, the mass transfer coefficient at the film free interface is obtained by

$$K = \frac{N_{Ay}|_{y=0}}{(C^*_A - C_{Ai})} = -\frac{DC}{\delta(C - C^*_A)}\frac{1}{\phi^*}\left.\frac{\partial\phi}{\partial Y}\right|_{Y=0}$$

$$\phi^* = \frac{C^*_A - C_{Ai}}{C^*_{Ai} - C_A}. \tag{34}$$

Utilizing equations (27) and (32) in equation (34), the corresponding local and average Sherwood numbers are obtained

$$Sh = \frac{Kz}{D} = A_1\frac{C\left(C - C^*_{Ai} + \frac{\sqrt{\pi}}{2}A_1 C\Lambda/\sqrt{(Le)}\right)}{(C - C^*_A)(C^*_A - C_{Ai})}\left(\frac{Z\,Pe^2}{4Le}\right)^{1/2} \tag{35}$$

$$\overline{Sh} = \frac{\bar{K}z}{D} = \frac{1}{z}\int_0^z Sh(z')\,\mathrm{d}z' = 2Sh. \tag{36}$$

The heat transfer coefficient due to non-isothermal absorption at the free interface is defined by

$$h = \frac{q|_{y=0}}{T^* - T_i} = -\frac{k}{\delta}\frac{1}{\theta^*}\left.\frac{\partial\theta}{\partial Y}\right|_{Y=0}. \tag{37}$$

Substituting the solution for the temperature profile given in equations (28)–(31) yields

$$h = \rho c_p\left[\frac{U_{max}\alpha}{\pi z}\right]^{1/2}. \tag{38}$$

The corresponding local and average Nusselt numbers are given by

$$Nu = \frac{hz}{k} = \left[\frac{Z}{\pi} Pe^2\right]^{1/2}; \quad \overline{Nu} = \frac{\bar{h}z}{k} = 2Nu. \quad (39)$$

3.1. *Convergence to the infinite dilution case*

In the case of absorption of sparingly soluble gases, $X_A \ll 1$, the terms of $(1-X_A)$ in equations (5) and (6) degenerate to 1 (or $\gamma\phi+\beta \to 1$). The formulation leading to equations (22)–(24) reduces to the known conventional heat and mass diffusion equations

$$Le\frac{d^2\phi^0}{d\xi^2} + 2\xi\frac{d\phi^0}{d\xi} = 0 \quad (40)$$

$$\frac{d^2\theta^0}{d\xi^2} + 2\xi\frac{d\theta^0}{d\xi} = 0 \quad (41)$$

with the corresponding boundary conditions

$$\xi \to \infty, \quad \phi^0 = 0, \quad \theta^0 = 0$$

$$\xi = 0, \quad \phi^0 + \theta^0 = 1$$

$$\xi = 0, \quad \frac{d\theta^0}{d\xi} = \Lambda\frac{d\phi^0}{d\xi}. \quad (42)$$

The analytical solutions to equations (40)–(42) have been given by Grigor'eva and Nakoryakov [12]

$$\phi^0 = \frac{\sqrt{(Le)}}{\Lambda+\sqrt{(Le)}}\{1-\mathrm{erf}\,(\xi/\sqrt{(Le)})\} \quad (43)$$

$$\theta^0 = \frac{\Lambda}{\Lambda+\sqrt{(Le)}}\{1-\mathrm{erf}\,(\xi)\}. \quad (44)$$

Based on equations (43) and (44), the local dimensional and non-dimensional mass and heat transfer coefficients, corresponding to infinite dilution, are given by

$$K^0 = \frac{-D(\partial C_A/\partial y)_{y=0}}{(C_A^* - C_{Ai})} = -\frac{D}{\delta}\frac{1}{\phi^*}\frac{\partial\phi}{\partial Y}\bigg|_{y=0} = \left[\frac{DU_{max}}{\pi z}\right]^{1/2} \quad (45)$$

$$h^0 = \frac{-k(\partial T/\partial y)_{y=0}}{(T^* - T_i)} = -\frac{k}{\delta}\frac{1}{\theta^*}\frac{\partial\theta}{\partial Y}\bigg|_{y=0} = \rho c_p\left[\frac{\alpha U_{max}}{\pi z}\right]^{1/2} \quad (46)$$

$$Sh^0 = \frac{k^0 z}{D} = \left[\frac{Z}{\pi}\frac{Pe^2}{Le}\right]^{1/2} \quad (47)$$

$$Nu^0 = \frac{h^0 z}{k} = \left[\frac{Z}{\pi} Pe^2\right]^{1/2}. \quad (48)$$

Comparison of equations (47) and (48) with equations (35) and (39) indicates that while the mass transfer coefficients at the film free interface for infinite and finite dilutions are different the heat transfer coefficients for the two cases are identical. This is in view of the fact that the temperature fields obtained by equations (28) and (44) are both described by error-function distribution. The constants in equations (28) and (44), however, are different, due to coupling with the mass transfer problem, which is affected by the dilution level $(1-X_A)$. Note also that both the heat and mass fluxes change with the dilution level due to the variation of the driving forces at the free interface.

The effect of finite dilution, as represented by $X_A = C_A/C \neq 0$ in equation (6), evolves from retaining the convective term in equation (4). An enhancement factor Ω is thus introduced, which expresses the ratio between the actual absorption mass transfer coefficient, K, and that obtained under the assumption of infinite dilution, K^0

$$\Omega = \frac{K}{K^0} = \frac{Sh}{Sh^0} = \frac{\sqrt{\pi}}{2}\frac{A_1\left(1-X_{Ai}^* + \frac{\sqrt{\pi}}{2}A_1\Lambda/\sqrt{(Le)}\right)}{(X_{Ai}^* - X_{Ai})(1-X_A^*)}. \quad (49)$$

It is also to be noted that the assumption of low absorption rate implies that $\rho\delta N_{A,y}/\Gamma C \ll 1$. In terms of Sh and Sh^0, as defined in equations (35) and (47), this restriction reads

$$\Omega = \frac{Sh}{Sh^0} \ll \frac{2\pi}{3}\frac{Sh^0}{(X_A^* - X_{Ai})} = \frac{2}{3}\frac{\sqrt{\pi}}{2(X_A^* - X_{Ai})}\left[\frac{z}{\delta}\frac{Pe}{Le}\right]^{1/2}. \quad (50)$$

A typical range of Pe/Le is 10^5–10^6. Calculated results (based on equations (27)–(33)) show that equation (50) is indeed satisfied.

4. RESULTS AND DISCUSSION

As is indicated by equations (27)–(33), the solution for the non-dimensional concentration of the absorbate is determined by both the interfacial concentration level (C_{Ai}^*/C) and the driving force $(C_{Ai}^* - C_{Ai})/C$. In the non-isothermal case, $\Lambda \neq 0$, and thus a third parameter, $\Lambda/\sqrt{(Le)}$, is involved. The calculated results are presented, in what follows, in terms of these three non-dimensional parameters. However, for the purpose of comparing θ and ψ for an identical ξ point, it is required to specify $\sqrt{(Le)}$ as well (see equations (27), (28) or (43) and (44)).

Figures 2–5 show the solutions for the dimensionless temperature and absorbate concentration distributions at various concentration levels, C_{Ai}^*/C, and specified nominal driving force, $(C_{Ai}^* - C_{Ai})/C$, or heat of absorption parameter, $\Lambda/\sqrt{(Le)}$. As is shown in Fig. 2, for large ξ (large y or small z) the temperature in the absorbing film is that of the inlet, therefore $\theta \to 0$. As the equilibrium concentration at the interface is higher than C_{Ai} due to the dilution caused by the process of condensation, the equilibrium inter-

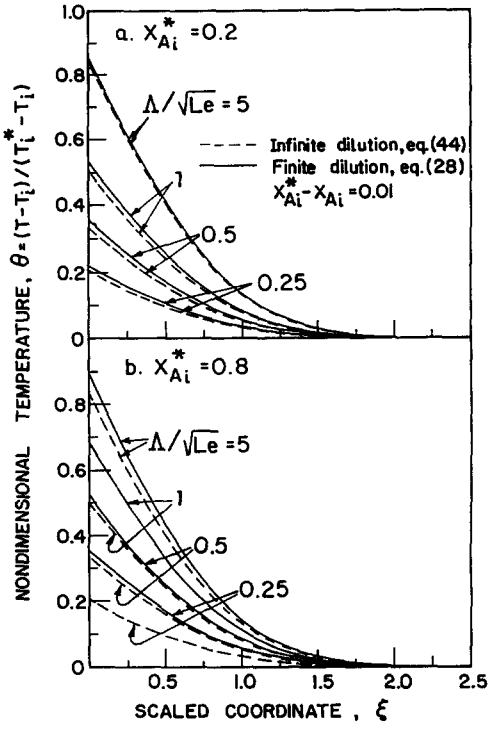

FIG. 2. Effect of absorbate concentration level on the temperature profiles.

facial temperature (for constant P_c) is always lower than T_i^*, hence θ at the interface ($\xi = 0$) is smaller than 1. For a relatively low concentration level ($X^*_{Ai} = 0.2$) the temperature profile approaches that for infinite dilution [10, 12] as given by equation (44) for all values of $\Lambda/\sqrt{(Le)}$. Increasing the concentration level, $X^*_{Ai} = 0.8$, as in Fig. 2(b), affects significantly higher interfacial temperature due to higher absorption rates (Fig. 6), thus θ deviates relative to that of infinite dilution, particularly at small ξ.

The absorbate distribution demonstrates similar trends as depicted in Figs. 3–5. For large ξ, the concentration goes to C_{Ai} or $\phi \to 0$, while at the interface, $\phi < 1$, indicating the effect of coupling between heat and mass transfer; if the temperature at the interface was constant at the entry level, T_i, as in isothermal absorption, the equilibrium interfacial concentration (with negligible pressure losses) would remain constant at C^*_{Ai}, or $\phi^* = 1$. This is demonstrated in Fig. 3(a) which relates to isothermal absorption, $\Lambda/\sqrt{(Le)} = 0$. As the concentration level increases, the solutions, in general, deviate from the low-penetration solutions for infinite dilution, equations (43) and (44), which under isothermal conditions reduce to Higbie's well-known solution [20]. For non-isothermal absorption, Figs. 3(b) and (c), the interfacial concentration, at $\xi = 0$, decreases with increasing concentration level, corresponding to the interfacial temperature rise noted in Fig. 2. However, for larger ξ, ϕ increases with increasing concentration level, indicating a deeper penetration of the diffusion boundary layer.

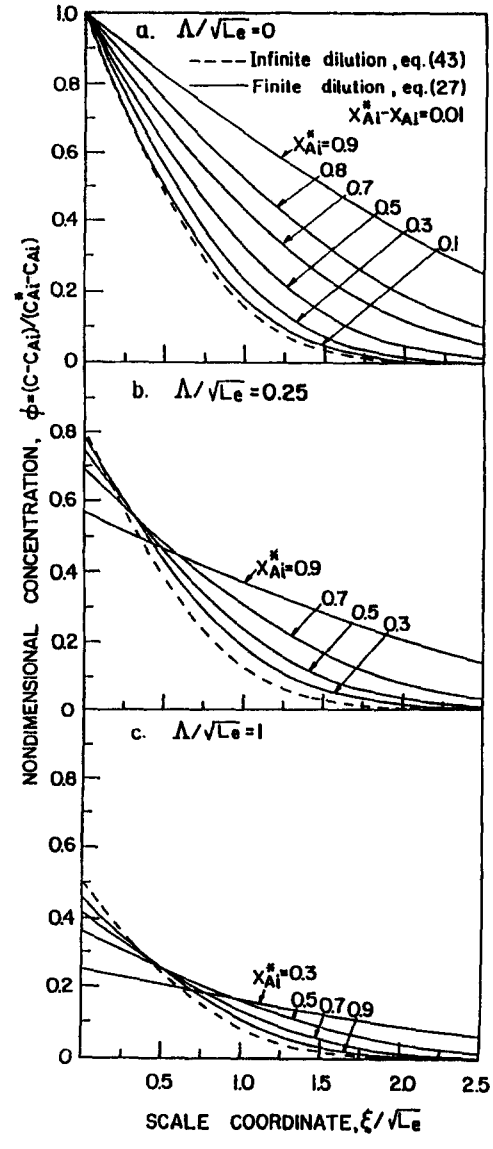

FIG. 3. Effect of absorbate concentration level on the concentration profiles.

The effect of heat and mass coupling parameter, $\Lambda/\sqrt{(Le)}$, is demonstrated through Figs. 2–4. For low heat of absorption or high Le, the heat interaction can be considered small (mass transfer controlled), and isothermal solutions are approached whereby $\theta \to 0$ (Fig. 2) and ϕ^* ($\xi = 0$) $\to 1.0$ (Figs. 3–5). As $\Lambda/\sqrt{(Le)}$ increases, the interfacial equilibrium temperature increases (Fig. 2) while the corresponding concentration decreases (Fig. 4). For high $\Lambda/\sqrt{(Le)}$, heat transfer dominates and therefore the effect of the concentration level diminishes (Figs. 2(a) and 4(b)). On the other hand, for lower $\Lambda/\sqrt{(Le)}$, where mass transfer dominates, the concentration level is of significant effect on both the temperature (Fig. 2(b)) and concentration (Fig. 4(b)) profiles as indicated by the

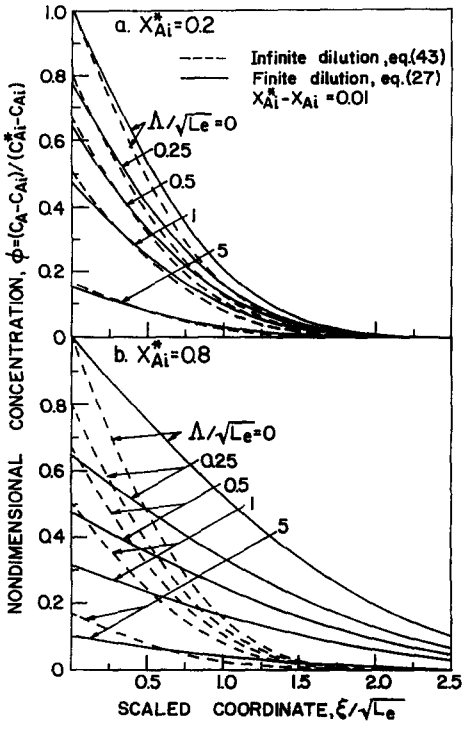

FIG. 4. Effect of coupling parameter on the concentration profiles.

deviation from the corresponding solutions for infinite dilution.

Figure 5 represents the interfacial concentration as functions of the coupling parameter and concentration level. Consistent with Figs. 2–4, the interfacial concentration decreases with both the concentration level and $\Lambda/\sqrt{(Le)}$. As is indicated by the figure, the solutions for finite dilution are bounded by that of infinite dilution, as given by equation (43) for $\xi = 0$. Note that $\theta^* = 1-\phi^*$.

The results presented so far relate the temperature and concentration profiles at constant driving force,

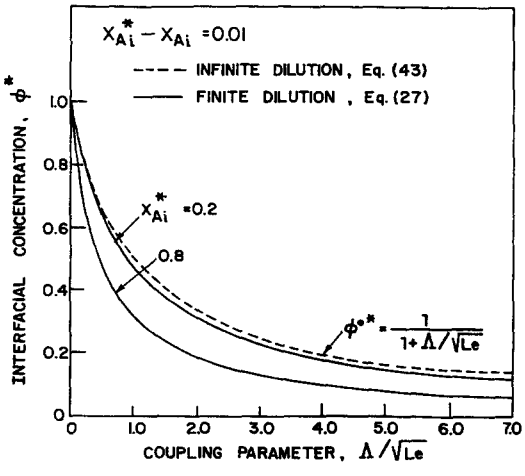

FIG. 5. Effect of concentration level and coupling parameter on interfacial concentration.

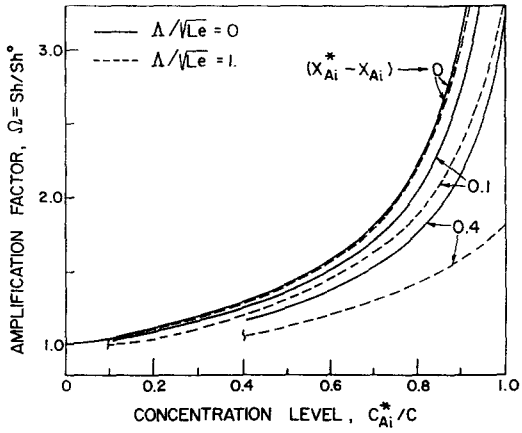

FIG. 6. Enhancement factor due to lateral convective term.

$(C^*_{Ai}-C_{Ai})/C = 0.01$. It has been found that the effects of the driving force on the θ, ϕ profiles are practically small and therefore are not shown here. On the other hand, the driving force has a significant effect on the transfer rates. This is presented by the enhancement factor, Ω, as defined in equation (49) and shown in Fig. 6. For a sufficiently low concentration level the transfer rate is close to that obtained for infinite dilution, and thus $\Omega \to 1$. However, as the concentration level increases (for constant $(C^*_{Ai}-C_{Ai})/C$, larger C^*_{Ai} corresponds to larger C_{Ai}) the enhancement factor exceeds 1.0, implying an enhanced transfer rate for finite dilution, both for the isothermal case $(\Lambda/\sqrt{(Le)} = 0)$ and non-isothermal conditions $(\Lambda/\sqrt{(Le)} > 0)$. As is indicated in Fig. 6, the enhancement factor is higher for the isothermal case, particularly for a large driving force, while for $(C^*_{Ai}-C_{Ai})/C \to 0$ the isothermal and non-isothermal solutions yield identical augmentation. Also to be noted, that increasing the driving force (for instance at constant C^*_{Ai}/C) is identical to decreasing the inlet concentration level, C^*_{Ai}/C, and thus approaching the conditions of infinite dilution, hence $\Omega \to 1.0$.

The increase in the transfer rate with increasing concentration level can be understood in view of equation (5), where both $(1-X_A)$ and the concentration gradient are included in the case of finite dilution. Inspection of Figs. 3–5 indicates, in fact, that a deterioration of the concentration gradients at the transferring interface $(\xi = 0)$ takes place as the absorbate concentration level increases. However, the transfer rate for finite dilution is determined by both the concentration gradient and the dilution term $(1-C^*_A/C)$, as indicated by equation (34). The enhancement factor, Ω, represents the augmentation of the mass transfer coefficient due to the inclusion of the convective term in equation (4). Therefore, it is evident that when high absorbate concentration levels are considered, neglecting the convection term may lead to significantly underpredicted absorption rates.

As the solutions presented herein are limited to low penetration condition $(u \simeq U_{max})$, it is of interest to

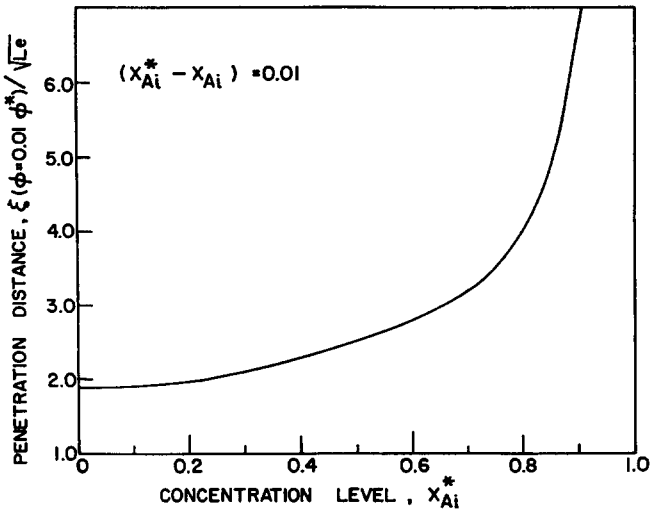

FIG. 7. Effect of concentration level on the penetration distance.

check the downstream distance where this assumption is still valid. For instance with a parabolic velocity profile, the velocity at the near-interface region deviates only 10% from U_{max} for $Y_{cr} = y_{cr}/\delta = 1/3$. Based on the definitions of ξ and equations (14), a given Y_{cr} corresponds to

$$Z_{cr} = \frac{z_{cr}}{\delta} \leqslant \frac{Re\,Sc}{4}\left[\frac{Y_{cr}}{\xi(\phi = 0.01\phi^*)}\right]^2 \qquad (51)$$

where $\xi(\phi = 0.01\phi^*)$ identifies the penetration of the diffusion boundary layer defined as that location where ϕ has dropped to 1% of the interfacial value. Figure 7 represents $\xi(\phi = 0.01\phi^*)$ vs the concentration level. Note that ξ for $\phi = 0.01\phi^*$ was found to be independent on the heat/mass coupling parameter. Consistent with the trends already shown in Figs. 3–5, increasing the absorbate concentration level results in an enhanced penetration of the diffusion boundary layer into the film. It should be kept in mind that the applicability of the solution is physically limited to z as given by equation (51). For example, at a concentration level of $X^*_{Ai} = 0.8$ Fig. 7 yields $\xi(\phi = 0.01\phi^*) \simeq 4$, and thus equation (51) for $Re\,Sc \simeq 10^6$ and $Y_{cr} = 1/13$ yields $Z_{cr} = z_{cr}/\delta < 1700$, beyond which the validity of the low penetration assumption becomes weak. Clearly for $X^*_{Ai} \to 0$, $\xi(\phi = 0.01\phi^*) \to 1.78$ as obtained by the error-function solution.

Finally, it is interesting to note the variation of the integration constant A_1 as obtained iteratively by equation (33) and shown in Fig. 8. Having the constant A_1, all other constants A_2, B_1, B_2 are easily determined by equations (30)–(32). Thus, the evaluation of A_1 from Fig. 8 may be helpful to estimate other calculated points not detailed in the previous figures.

5. FINAL REMARKS

It has been shown that in physical systems where the absorbate concentration level is finite and is comparable to that of the absorbent component, as in hygroscopic condensation, the convective term in the lateral direction is to be accounted for. The inclusion of the convective term is of importance as it results in enhanced transfer rates. Therefore, the use of empirical correlations, or models, obtained for an infinite absorbate dilution, may yield conservative transfer rates in the design of hygroscopic condensation evaporation systems [1–6].

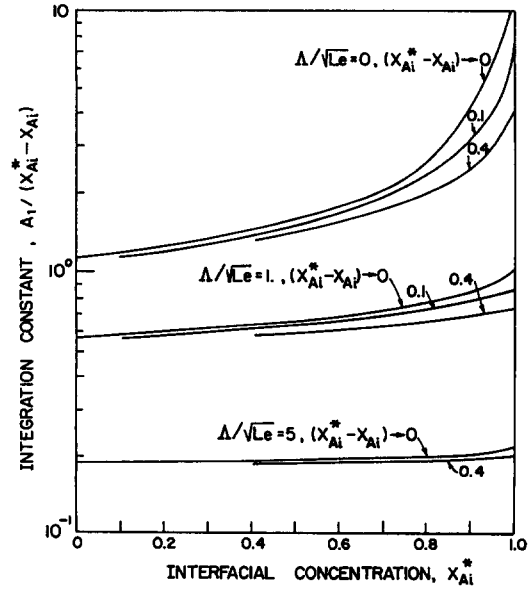

FIG. 8. Effect of various operating conditions on the integration constant, A_1.

REFERENCES

1. D. Moalem Maron and N. Brauner, Analysis of power cycle based on absorption evaporator–condenser, Rept No. 1, Proj. 0251, Faculty of Engineering, Tel-Aviv University, submitted to Ormat Turbines, Ltd, Sept. (1983).
2. N. Brauner and D. Moalem Maron, Hygroscopic condensation–evaporation power cycle, Rept No. 3, Proj.

0251, Faculty of Engineering, Tel-Aviv University, submitted to Ormat Turbines, Ltd, March (1985).
3. N. Brauner, D. Moalem Maron and S. Sideman, Heat and mass transfer in direct contact hygroscopic condensation, *Proc. 8th Int. Heat Transfer Conf.*, San Francisco, Vol. 4, pp. 1647–1652 (1986).
4. N. Brauner, D. Moalem Maron and S. Sideman, Heat and mass transfer in direct contact hygroscopic condensation, *Wärme- und Stoffübertr.* **21,** 233–245 (1987).
5. N. Brauner, D. Moalem Maron, Z. Harel and S. Sideman, Hygroscopic film condenser–evaporator heat cycle, thermal-hydraulic fundamentals and design of two-phase flow heat exchangers, *Proc. Nato Advanced Study Institute*, Portugal (1987).
6. N. Brauner, D. Moalem Maron, Z. Harel and S. Sideman, Power recovery of concentration based energy sources by direct contact hygroscopic condensation on brine films, energy storage systems: fundamentals and applications, *Proc. Nato Advanced Study Institute*, Cesme-Izmir, Turkey (1988).
7. A. Bakopoulos, Liquid-side controlled mass transfer in wetted-wall tubes, *Germ. Chem. Engng* **3,** 241–252 (1980).
8. A. K. Bin, Mass transfer into turbulent liquid film, *Int. J. Heat Mass Transfer* **26,** 981–991 (1983).
9. S. M. Yih and K. Y. Chen, Gas absorption into wavy and turbulent falling liquid films in a wetted wall column, *Chem. Engng Commun.* **17,** 123–136 (1982).
10. G. Grossman, Heat and mass transfer in film absorption. In *Handbook of Heat and Mass Transfer* (Edited by N. P. Chezemisinoff), pp. 211–258. Gulf, Houston (1986).
11. S. M. Yih and R. C. Seagrave, Mass transfer in laminar falling liquid films with accompanying heat transfer and interfacial shear, *Int. J. Heat Mass Transfer* **23,** 749–758 (1980).
12. N. I. Grigor'eva and V. E. Nakoryakov, Exact solution of combined heat and mass transfer problem during film absorption, *Inzh.-fiz. Zh.* **33,** 983–989 (1977).
13. V. E. Nakoryakov and N. I. Grigor'eva, Calculation of heat and mass transfer in non-isothermal absorption in the entrance region of a falling film, *Teor. Osn. Khim. Tekhnol.* **14,** 483–488 (1980).
14. G. Grossman, Simultaneous heat and mass transfer in film absorption under laminar flow, *Int. J. Heat Mass Transfer* **26,** 357–371 (1983).
15. G. Grossman and M. T. Heath, Simultaneous heat and mass transfer in absorption of gases in turbulent liquid films, *Int. J. Heat Mass Transfer* **27,** 2365–2376 (1984).
16. H. Le Goff, A. Ramadane, M. Barkaoui, Y. Chen and P. Le Goff, Modelling the coupled heat and mass transfer in falling film application to absorbers and desorbers in absorption heat pumps, *Proc. 8th Int. Heat Transfer Conf.*, San Francisco, Vol. 4, pp. 1971–1976 (1986).
17. N. Brauner, D. Moalem Maron, Z. Harel and S. Sideman, Hygroscopic film condensation/evaporator unit, *Proc. Inst. Mech. Engrs*, U.K. Heat Transfer Conf., Glasgow (1988).
18. N. Brauner, D. Moalem Maron and H. Meyerson, The effect of absorbate concentration level in hygroscopic condensation, *Commun. Heat Mass Transfer* **15**(3), 269–279 (1988).
19. W. F. Ames, *Nonlinear Partial Differential Equations in Engineering*. Academic Press, New York (1965).
20. R. Higbie, Rate of absorption of gas into a still liquid, *Trans. A.I.Ch.E.* **31,** 365–389 (1935).

COUPLAGE DE L'ABSORPTION DE MASSE ET DE CONDENSATION THERMIQUE AVEC DES CONCENTRATIONS COMPARABLES D'ABSORBAT ET D'ABSORBANT

Résumé—L'absorption de gaz modérément solubles est conventionnellement caractérisée par une dilution infinie de l'absorbat. La présente étude concerne l'absorption de vapeur lorsque les concentrations d'absorbat et d'absorbant sont comparables (dilution finie de l'absorbat). Un tel mécanisme est, par exemple, la condensation hygroscopique de vapeur à faible pression sur un film chaud tombant de saumure. On considère les absorptions isothermes et non isothermes avec couplage de transfert de chaleur et de masse. On montre que dans le cas d'une dilution finite, le terme convectif latéral doit être pris en compte. Les flux résultants de transfert dépendent à la fois du niveau de concentration de l'absorbat et de la force motrice et ils sont sensiblement accrus par rapport à ce que prédit la théorie de Higbie.

GEKOPPELTE KONDENSATION UND ABSORPTION BEI VERGLEICHBARER KONZENTRATION DES ABSORBIERTEN UND DES ABSORBIERENDEN STOFFES

Zusammenfassung—Die Absorption von schlecht lösbaren Gasen ist gewöhnlich durch die unbegrenzte Verdünnung des absorbierenden Stoffes bestimmt. Die vorliegende Arbeit befaßt sich mit der Absorption von Dampf, bei der die Konzentrationen des absorbierten und des absorbierenden Stoffes vergleichbar sind (begrenzte Verdünnung des absorbierten Stoffes). Ein solcher Vorgang ist zum Beispiel die hygroskopische Kondensation von kaltem Niederdruckdampf an einem Rieselfilm aus heißem konzentriertem Salzwasser. Es wird die isotherme und die nicht-isotherme Absorption betrachtet, wobei im zweiten Fall gekoppelte Wärme- und Stoffübertragung auftritt. Es zeigt sich, daß im Falle einer begrenzten Verdünnung der Term für die quergerichtete Konvektion in Betracht gezogen werden sollte. Die Stoffübertragung hängt offensichtlich sowohl von der Konzentration des absorbierten Stoffes als auch von der treibenden Kraft ab. Sie ist deutlich besser, als dies die Theorie von Higbie beschreibt.

СВЯЗАННЫЕ ПРОЦЕССЫ ТЕПЛОВОЙ КОНДЕНСАЦИИ И ПОГЛОЩЕНИЯ ВЕЩЕСТВА ПРИ СОПОСТАВИМЫХ КОНЦЕНТРАЦИЯХ АБСОРБАТА И АБСОРБЕНТА

Аннотация—Поглощение слаборастворимых газов характеризуется неограниченным разбавлением абсорбируемого вещества. В данной работе исследуется поглощение пара с соизмеримыми уровнями концентрации абсорбируемого и абсорбирующего веществ (ограниченное разбавление абсорбата). Таким процессом является, в частности, гигроскопическая конденсация холодного пара при низком давлении на стекающей пленке горячего концентрированного раствора соли. Рассматриваются изотермические и неизотермические поглощения—процессы, представляющие собой связанный тепло- и массоперенос. Показано, что в случае ограниченного разбавления следует учитывать член, описывающий поперечную конвекцию. Установлено, что найденные скорости тепло- и массопереноса зависят как от уровня концентрации абсорбируемого вещества, так и от движущей силы и что они намного выше значений, рассчитываемых по теории Хигби.